Transportation Geotechnics 46 (2024) 101267

Contents lists available at ScienceDirect

Transportation Geotechnics

journal homepage: www.elsevier.com/locate/trgeo

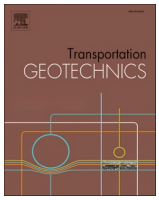

Original Article

Subgrade soil response to rail loading: Instability mechanisms, causative factors, and preventive measures

Buddhima Indraratna [a,*], Thanh T. Nguyen [b], Shashika Atapattu [b], Trung Ngo [b], Cholachat Rujikiatkamjorn [b]

[a] Distinguished Professor of Civil Engineering and Director of Transport Research Centre, University of Technology Sydney, Ultimo, Australia
[b] Transport Research Centre, School of Civil and Environmental Engineering, University of Technology Sydney, Ultimo, Australia

ARTICLE INFO

Keywords:
Fluidisation
Instability mechanisms
Rail loading
Subgrade soil
Vertical drain

ABSTRACT

The demand for more efficient heavy-haul rail networks over soft subgrades poses significant geotechnical challenges and requires a comprehensive understanding of stress conditions as well as the failure potential of subgrade soil under moving wheel loads and increasing rail speeds. Unfavourable stress conditions in the subgrade can result in various types of failures, three of which are identified in this article: (i) excessive plastic settlement, (ii) progressive shear failure, and (iii) subgrade fluidisation (mud pumping). Through a series of advanced testing schemes using cyclic triaxial, hollow cylinder, and an in-house dynamic filtration apparatus, critical stress conditions and soil characteristics prone to subgrade instability are discussed. The results demonstrate that under adverse combinations of loading frequency (f) and cyclic stress ratio (CSR) the continuous application of cyclic loads can lead to an unstable state of soil where excess pore pressure and axial strain increase rapidly. This study also reveals that low to medium plasticity soils (PI < 22) are more vulnerable to subgrade fluidisation, where the rapid internal migration of pore water transforms the upper soil to a fluid-like state with substantial loss in soil stiffness. The layered response of soil through dynamic filtration tests showed larger hydrodynamic forces induced by differential hydraulic gradients in the top layer during cyclic loading causes moisture to move upwards. Various factors that can influence soil instability such as the degree of compaction degree, clay content, soil fabric and stress rotation are also addressed in this paper. Finally, novel solutions for stabilising subgrade such as a vertical drain-composite system and the use of eco-friendly biopolymers are presented.

Introduction

The Australian heavy haul railway, among the world's largest, spans 32,567 route-kilometre and transported 445.3 billion tonne-kilometres of freight in 2022–23 (BITRE 2023). Despite its vast network and locomotives capable of carrying axle loads from 16 to 42 tonnes over lengths exceeding 4 km, the system often fails to meet the demand from industries such as mining and agriculture. To address these requirements, the Inland Rail network (to be completed by 2027) will connect the Melbourne to Brisbane route with a 1,700-kilometer track designed for an average axle load of 21 tonnes and a maximum speed of 115 km/h. However, geological conditions such as soft alluvium in floodplain regions pose significant geotechnical obstacles, while increased rainfall due to climate change has further amplified flooding and wet soil regions along the route, urging thorough research efforts and design methods for a more resilient track foundation.

Understanding the development and propagation of dynamic stresses beneath rail tracks is vital for addressing subgrade-related issues. Rail track structure typically includes rails, sleepers, ballast, sub-ballast, and subgrade (Fig. 1). The dynamic stresses generated from rail loads move from sleepers to subgrade and exhibit significant variations in magnitude and direction during train passage, along with high concentrations of stress. While ballast primarily mitigates the transfer of stress to the subgrade, the dynamic nature of stress and its impact on how soil responds warrants further investigation.

Various methods such as numerical simulations [56,15,61,72], full-scale laboratory models [9,30] and field investigations [31,57] have been used to understand stress behaviour in subgrade soil. Field measurements at Bulli, NSW, Australia, revealed a maximum cyclic stress of 70 kPa applied to the subgrade soil [31], while a combined field and

* Corresponding author.
E-mail address: buddhima.indraratna@uts.edu.au (B. Indraratna).

https://doi.org/10.1016/j.trgeo.2024.101267
Received 19 March 2024; Received in revised form 28 April 2024; Accepted 4 May 2024
Available online 9 May 2024

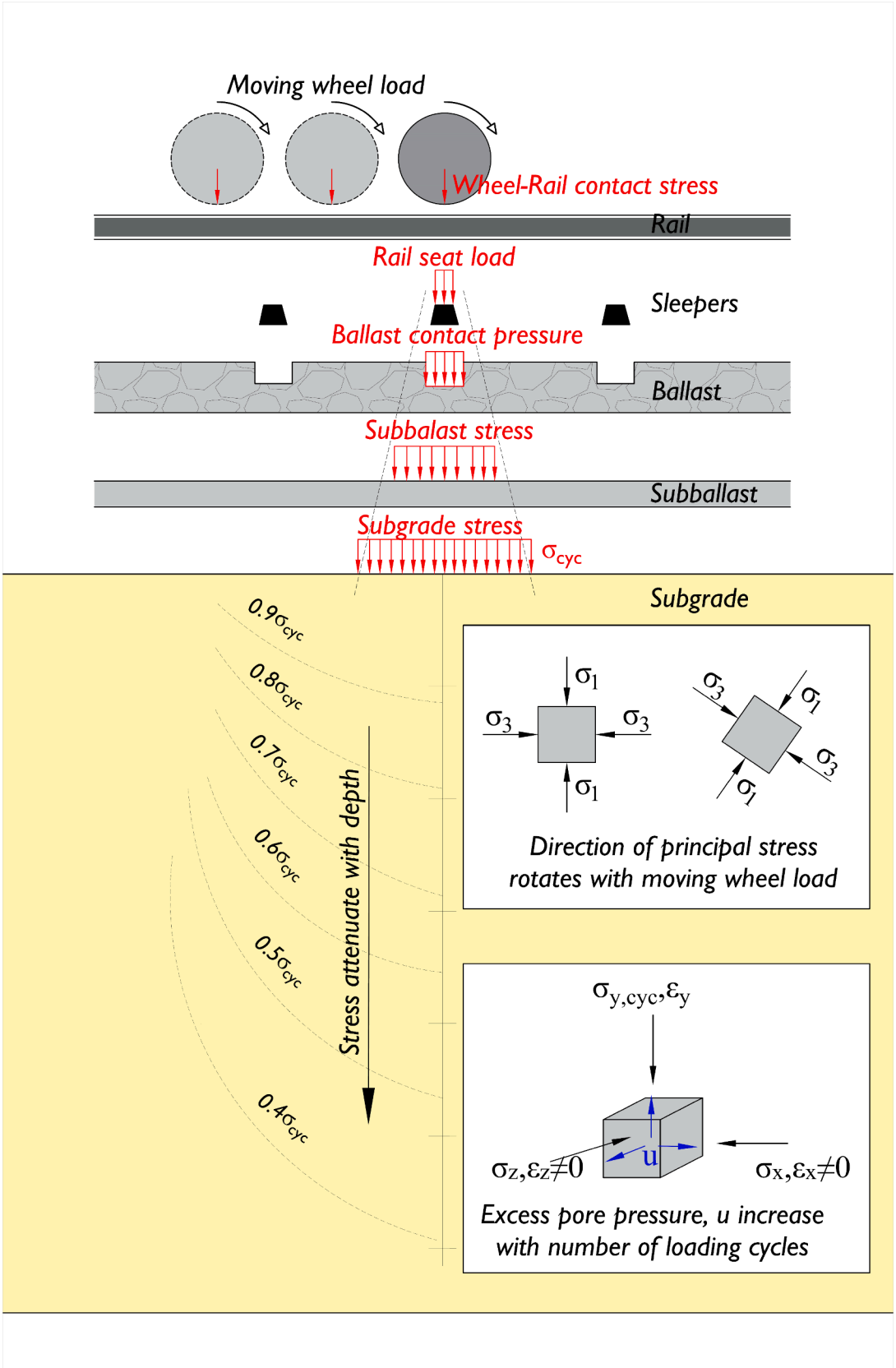

Fig. 1. Complex dynamic behaviour of stress in subgrade induced by train passage.

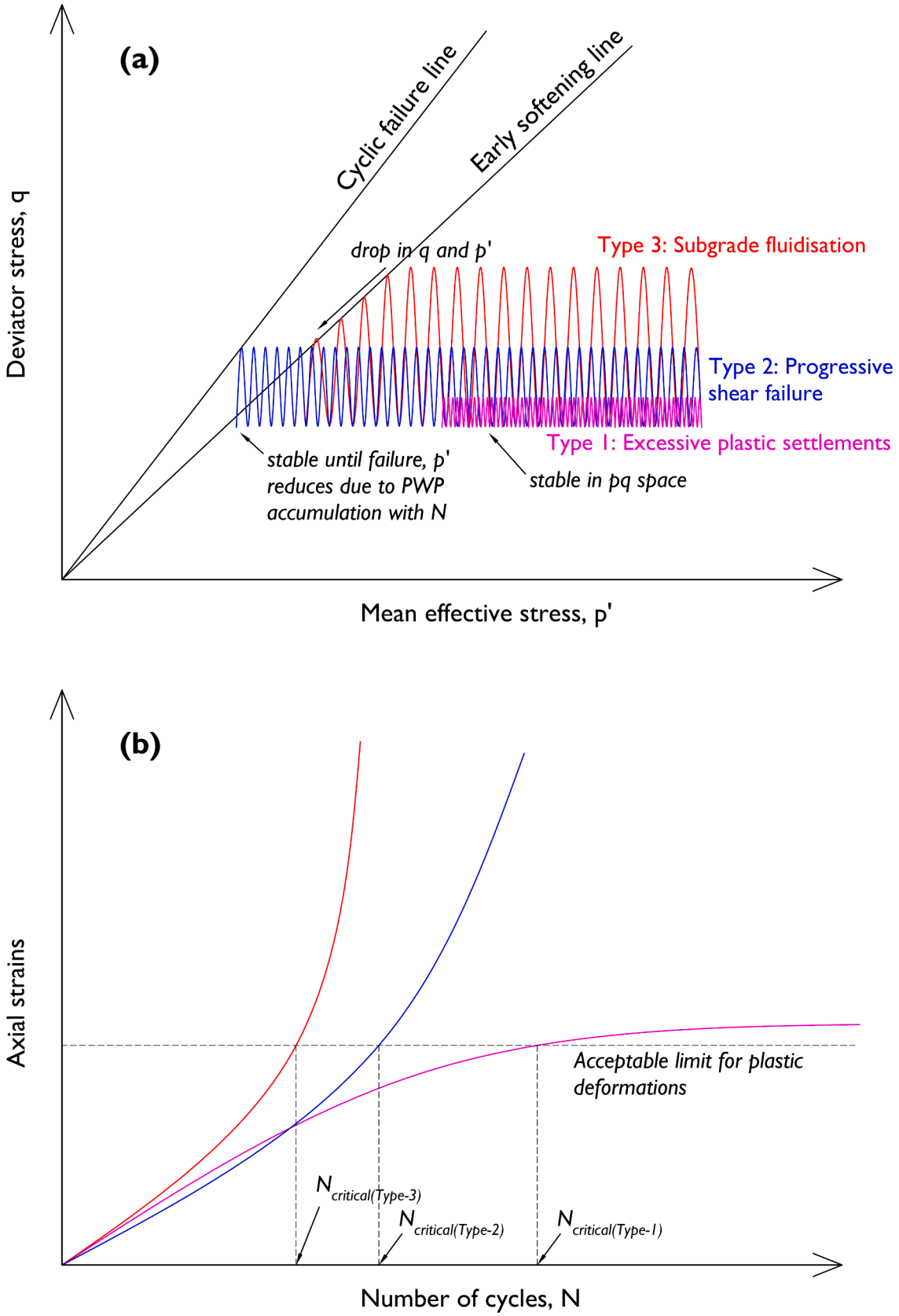

Fig. 2. Typical failure modes of subgrade soil under cyclic loading: a) stress path in p'-q plane and b) axial strain over loading cycles N.

numerical investigation by Priest et al. [57] reported that the vertical stress in shallow subgrade (780 mm below sleeper) could reach 80 kPa under an axle load of 26 tonnes. Numerical simulations by Powrie et al. [56] and Mamou et al. [47] indicated various frequencies acting on ballast, reporting a frequency of 4.0 Hz at 1.0 m below the sleeper base from a train travelling at 180 km/h. Experiments using large-scale prototype railway tracks provided insights into stress distribution at different depths under diverse scenarios. For instance, a 1:1 scale prototype by Indraratna et al. [30] showed that a 25-tonne axle load resulted in a maximum vertical stress of approximately 225 kPa at the sleeper-ballast interface, which then decreased rapidly with depth. A maximum vertical stress at the subgrade surface was recorded at 95 kPa, which then decreased to 48 kPa at a depth of almost 800 mm.

The instability of subgrade soil under railways has garnered a lot of attention, with research identifying three major failure mechanisms: excessive plastic deformation, progressive shear failure, and subgrade fluidisation.

Excessive plastic settlement (Type-1)

The subgrade remains stable but cyclic loading leads to unfavourable track settlement due to undrained shear deformation or volumetric strain [41–42]; equilibrium is eventually reached as the excess pore water pressure stabilises. Although consolidation and creep settlements contribute to track settlements under static loading, it is widely accepted that cyclic loading can accelerate plastic deformation [12,5,11]. Thus, plastic settlements induced by cyclic loading were assessed under different stress states and load combinations, as well as capturing varying soil properties. For example, the role of stress state considering the initial confining pressure and stress anisotropy was investigated by Leng et al. [40] and Tong et al. [70]. Other studies have demonstrated the influence of loading frequency (i.e. representing the train speed) on the accumulated strain based on triaxial test results [45,71,73,65]. Initial water content and compaction quality were also reported as decisive factors contributing to significant plastic deformation of soft subgrade soil [45,40]. Furthermore, results obtained from cyclic triaxial and hollow cylindrical testing have shown that moving load and corresponding principal stress rotation can generate increased plastic settlement [23,74,24]. For instance, Gräbe and Clayton [22] suggested that the rate of increase in plastic strain resulting from the principal stress rotation was inversely proportional to the clay content of the subgrade (clay contents varying from 7 to 24 %). More recently, the effects of intermittent cyclic loading representing the rest periods between train passages were considered, where the drainage conditions and cyclic stress magnitudes played a pivotal role in the development of subgrade settlement [39,44,7,27].

Progressive shear failure (Type-2)

The stress path gradually approaches the failure envelope with increasing loading cycles, which leads to sudden and unacceptable deformation in the subgrade as the mean effective stress decreases due to the accumulation of excess pore pressure [41]. This situation primarily arises when the drainage in the subgrade is poor, leading to the accumulation of excess pore pressures due to sustained cyclic shear stresses [2]. In soils of relatively high permeability (e.g. gravels and sands), fully drained conditions can be expected with insignificant excess pore pressures, while in low-permeability soils with high fines content, considerable increase in excess pore pressure occurs under undrained conditions [55]. Mamou et al. [48] showed that increasing the clay content from 7 % to 14 % in a saturated sand-clay mixture could reduce excess pore pressures and increase the cyclic shear stress threshold. However, increasing the clay content to 24 % and beyond resulted in an increase in excess pore pressure with insignificant effect on the cyclic shear stress threshold. Fedakar et al. [19] demonstrated that the influence of principal stress rotation can become increasingly pronounced for higher clay contents based on the results obtained from cyclic triaxial and hollow cylinder tests. For example, for a clay content 20 %, shear strain developed rapidly with strain softening at a small number of loading cycles (N ⟨500).

Subgrade fluidisation (Type-3)

Accumulated excess pore pressure results in a hydraulic gradient which causes fine particles to migrate upwards and form a slurry at the surface layers [35]. This can lead to sudden and unacceptable increases in strain that is characterised by early stiffness degradation and strain-softening in the soil. Physical model tests [17,13,4,16] successfully reproduced the phenomenon of upward migration of fluidised soil under cyclic loading.

Each type exhibits distinct stress–strain patterns in the p'-q plane, as illustrated in Fig. 2. While Types 1 and 2 have been studied extensively over the past three decades, mud pumping as a phenomenon has garnered rapidly increasing attention in recent years despite it being a longstanding issue in rail track foundations [58,62,8,63,13,26,51]. This heightened interest is attributed to the global surge in the development of rail transportation and the enduring mystery surrounding the failure mechanism of mud pumping soil. The questions surrounding how soil particles migrate upwards under cyclic loading and the key factors influencing this process remain unanswered. Field reports and experimental studies on mud pumping often lack measurements such as the internal water content, and localised stress, and pore pressure can hinder our understanding of the triggering conditions. Moreover, the reduction in shear strength and changes in its constitutive behaviour due to the loss of soil mass during mud pumping present critical issues for study, as highlighted in the recent studies of stiffness degradation of soil prone to mud pumping [67]. To unravel the complex mechanism of mud pumping, sophisticated experimental models accompanied by advanced computational simulations are essential, especially considering the intricate combination of layer-scale and elemental concepts involved.

Several soil stabilisation methods have been developed and successfully applied to track foundations. One fundamental approach to mitigating high dynamic stress in the subgrade is to minimise its propagation by increasing ballast thickness and having high embankments. While these methods are commonly used, they often require large material resources which poses challenges due to the scarcity of resources. Geosynthetics like geogrids and geotextiles have been used for decades to successfully reinforce railway foundations, and for very soft soils, cementation techniques such as deep mixing and jet grouting can significantly enhance the shear strength of subgrade soil before the placement of ballast. However, these methods often rely on fossil-based materials which contribute to greenhouse gas emissions and environmental degradation. In some cases, geotextiles alone have been unable to stop mud pumping, as indicated by site investigations [63,10,50,52]. Degraded permeability and serious deterioration have occurred, highlighting the need for new, eco-friendly, and cost-effective solutions to enhance stability and robustness in subgrade foundations, as well as the remediation of mud pumping.

This paper presents the essence of state-of-the-art research conducted in recent times at the Transport Research Centre (TRC), University of Technology Sydney (UTS), focusing on the evolution of stress in soft subgrade layers and its impact on cyclic soil instability. Advanced numerical analysis using 3D Finite Element Method (FEM) was used to study the development of stress under moving wheel loads and increasing rail speeds, crucial knowledge for understanding the complex behaviour of stress in subgrade soil. Laboratory tests such as cyclic triaxial and hollow cylinder tests, as well as dynamic filtration apparatuses, were carried out to examine soil instability induced by fluidisation, particularly in soils prone to mud pumping. The influence of various factors such as load combinations, the degree of compaction, soil plasticity, soil fabric and stress rotation were investigated. Novel and emerging solutions for stabilising mud pumping in rail tracks such as

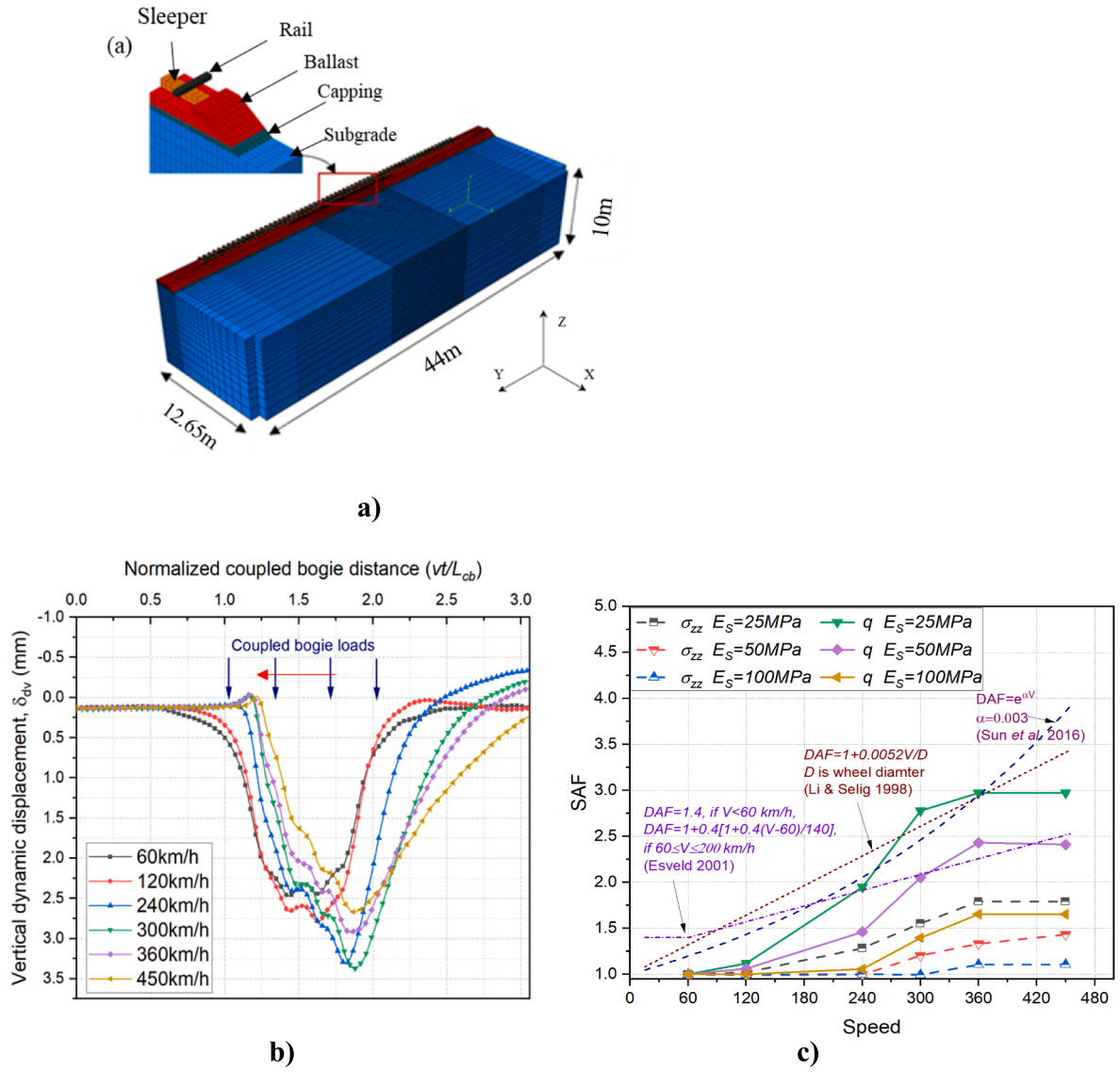

Fig. 3. a) 3D FE ballasted track model; b) dynamic vertical displacement in the ballast at various speeds; and c) Vertical and deviator stress amplifications and comparison against empirical relationships from past literature (modified after [72]).

advanced geocomposites and biopolymers are also presented. This research contributes to a comprehensive understanding of subgrade soil instability and offers innovative preventive techniques to enhance the practical design of rail track foundations.

Stress evolution in subgrade soil under moving axle loads: 3D FEM analysis

Finite Element Modelling

Numerical simulations based on Finite Element Method (FEM) were implemented to investigate the variation of stress in subgrade under moving wheel loads. Fig. 3a illustrates the dimensions of the 3D mesh discretisation that captures the steel rails, concrete sleepers, a 300 mm thick layer of ballast, and a 150 mm thick compacted capping layer (sandy gravel) above a natural 10 m deep subgrade (silty clay). To optimise computational efficiency the double symmetry of the track was exploited, allowing for the analysis of half the track with a single steel rail in the transverse y-z plane. The rail is represented as a solid section with a standard 60 kg/m profile at a spacing of 1.435 m along the longitudinal direction. The concrete sleepers follow typical Australian standard gauge dimensions, i.e. 2.5 m long, 260 mm wide and 230 mm thick. Further details of the model can be found in Tucho et al. [72].

Material models and parameters

The steel rails and concrete sleepers are modelled as small-strain linear-elastic materials. For dynamic analysis of railway ballast under cyclic loading the non-associative Drucker-Prager (D-P) model was used. The strength, deformation, and damping parameters were derived from extensive monotonic and cyclic triaxial tests [33]. The capping and subgrade layers are represented using an elasto-plastic model adopting the Mohr-Coulomb yield condition where the subgrade is assumed to be a lightly over-consolidated silty clay. The mechanical properties of the track material were selected from literature published for this study [25,33], as presented in Table 1. The boundary along the plane of symmetry restricted the lateral (transverse) displacement parallel to the sleeper, while other domain edges were modelled as infinite elements (element type: CIN3D8) to reduce model disturbance from residual-by-residual waves at the boundaries [14,37,64]. Overall, the discretised mesh consists of 152,685 nodes and 132,911 hexahedral elements (element type: C3D8R).

Table 1
Material parameters adopted in the FEM analysis (data).

Track Components	Value
Rail	
Density (kg/m^3)	7850
Young's modulus (MPa)	210,000
Poisson's ratio, ν	0.3
Sleeper	
Density (kg/m^3)	2500
Young's modulus (MPa)	30,000
Poisson's ratio, ν	0.25
Ballast	
Density (kg/m^3)	1530
Young's modulus (MPa)	200
Poisson's ratio, ν	0.3
Cohesion (kPa)	1
Friction angle, ϕ (degrees)	50
Dilation angle, ψ (degrees)	20
Capping	
Density (kg/m^3)	1800
Young's modulus (MPa)	150
Poisson's ratio, ν	0.3
Cohesion (kPa)	1
Friction angle, ϕ (degrees)	35
Dilation angle, ψ (degrees)	5
Subgrade	
Density (kg/m^3)	1730
Young's modulus (MPa)	50
Poisson's ratio, ν	0.35
Cohesion (kPa)	30
Friction angle, ϕ (degrees)	24
Thickness (m)	10
R-Wave velocity, V_R (km/h)	342

Source: [72]

The viscous damping in each track component was implemented through Rayleigh damping models in FE analysis and consist of a damping matrix [C], a mass matrix [M], stiffness matrix, K [36]:

$$[C] = \alpha[M] + \beta[K] \tag{1}$$

where the coefficients α and β are given by:

$$\begin{Bmatrix} \alpha \\ \beta \end{Bmatrix} = \frac{2D}{\omega_1 + \omega_2} \begin{Bmatrix} \omega_1\omega_2 \\ 1 \end{Bmatrix} \tag{2}$$

where D is the damping ratio and ω_1 is the resonant frequency of the subgrade, and ω_2 is considered as the frequency of the wheel passage that defines the damping curves in rad/s.

Predicted stress-displacement responses

Fig. 3 presents the dynamic vertical deflection at the centre of the ballast layer with the increased train speeds. The horizontal axis is normalised to a coupled-bogie distance (vt/L_{cb}) to depict the results across different speeds on a uniform scale where v is the train speed, t is the total simulation time for the load to traverse the model, and L_{cb} is the length of the two bogies. The results indicate that vertical deflection under a moving wheel load increases with the train speed until it reaches 300 km/h, beyond which there was a noticeable decline in dynamic displacement (δ_{dv}). Considering the peak displacement response, a train speed nearing 300 km/h (approximately 0.9VR) can be deemed the critical speed for the track-subgrade properties considered in the finite element analysis.

Stress amplification

The effects of train speed and subgrade modulus on the deviator and stress amplification factor (SAF) are presented in Fig. 3. The SAF is defined as the ratio of stress response at any speed to the quasi-static response at 60 km/h. The changes in deviator (q), mean (p), and vertical (σ_{zz}) stress induced by a moving wheel load can be approximated as follows:

$$p' = \frac{\sigma_{xx} + \sigma_{yy} + \sigma_{zz}}{3} \tag{3}$$

$$q = \sqrt{\frac{1}{2}\left((\sigma_{xx} - \sigma_{yy})^2 + (\sigma_{yy} - \sigma_{zz})^2 + (\sigma_{zz} - \sigma_{xx})^2\right) + 3\left(\tau_{xy}^2 + \tau_{yz}^2 + \tau_{zx}^2\right)} \tag{4}$$

The results (Fig. 3) show that the vertical and deviator stress amplification decreases as the subgrade modulus (E_s) increases. The predicted SAF for deviator stress (q) decreases from 2.98 to 1.7, while for vertical stress (σ_{zz}), it decreases from 1.8 to 1.1 when the subgrade modulus increases from 25 MPa to 100 MPa. Moreover, the vertical stress experiences less amplification than the corresponding deviator stress across all the subgrades and train speeds considered.

Furthermore, the predicted SAF are compared to empirical models of dynamic amplification factor (DAF) derived from earlier studies such as Esveld [18], Li and Selig [43]. Notably, Li and Selig [43] and Sun et al. [69] offered a conservative estimate of DAF except where a train is moving faster than 300 km/h on a track situated on a relatively soft formation. In contrast, the method proposed by Esveld [18] underestimates stress amplification at speeds higher than 240 km/h, while providing significantly higher amplification for lower to medium-speed ranges (<240 km/h) when the subgrade modulus is 50 MPa and 100 MPa. These results indicated that when train speed increases from 60 to 300 km/h the dynamic deviator stress in the subgrade layer can develop rapidly in a non-linear manner with a DAF that can exceed two at a speed of 240 km/h.

In conventional track design, the dynamic stresses induced by train passage are determined by multiplying DAF to the static loading. This factor is often used in practice to consider the effect of train speed and track irregularity [18]. It is noted that the variations of stress experienced by a soil element below a rail track are highly complex because of the dynamic interaction between the train and the track substructure, involving rotation of the principal stress directions [56]. In addition, Rayleigh wave effects can cause an amplification of stresses and displacements upon train passage. In this study, a moving train loading was simulated by applying a vertical load (P) to a rigid body at the top of the rail, which was then horizontally displaced at a constant speed. This method has been validated for complex analyses, including vehicle-bridge interactions and dynamic load assessments [46,60].

The instability of subgrade soil examined through experimental investigation

Experimental consideration

The failure of subgrade soil under rail tracks has received a lot of attention over the years, and the experimental studies have made significant contributions to understanding the mechanism. Experimental studies can be classified into four different categories:

(i) Element tests using a single and homogeneous material such as cyclic triaxial and hollow cylinder apparatuses,
(ii) Large-scale cyclic tests where the layered response of soil can be observed and measured under an axial load,
(iii) Full-scale rail track model where different layers of track foundations and multiple axial loads can be replicated,

Fig. 4. Site investigation on subgrade failure and sample collection for laboratory studies: a) site observations and b) properties of soils prone to mud pumping.

(iv) Field-scale tests where monitoring and measurements occur at the actual sites.

To understand the failure mechanisms, element and large-scale tests are usually preferred. This section reports on recent findings based on these model tests, with special reference to soil fluidisation and the associated internal instability of subgrade under cyclic loading.

Collections of soil samples in mud pumping sites and laboratory testing

An extensive site investigation on twenty mud pumping spots along the South Coast rail line (NSW, Australia) was carried out from 2019 – 2022 [50,52], to assess the field conditions that cause mud pumping and to obtain soil samples for laboratory examination (Fig. 4). The soil samples were taken from shallow layers, often 1–2 m deep subgrade. Triaxial (TT) and hollow cylinder (HC) tests were used to explore the behaviour of reconstituted samples under different stress states and loading conditions; they are described later in this paper. The results showed that all the subgrade soils can be classified as low plasticity clay (CL) with a plasticity index (PI) < 22. The site investigation found poor drainage conditions, which were either induced by improper design of drainage systems or considerable fouling of the ballast/subballast layers which imposed undrained or strictly limited drainage conditions that can trigger mud pumping under railways.

Cyclic test procedures

The general procedure for preparing reconstituted specimens for both tests is as follows: the soil samples were dried and then mixed with distilled water at the optimum water content determined by compaction tests. The under-compaction method was used to ensure a uniform density and thus porosity. Solid cylindrical specimens 50 mm diameter by 100 mm high were made for the triaxial tests, and hollow cylindrical specimens 100 mm outside diameter (60 mm inside diameter) by 200 mm high were prepared for the hollow cylinder test. For low to medium plasticity soils which often have optimum moisture content for

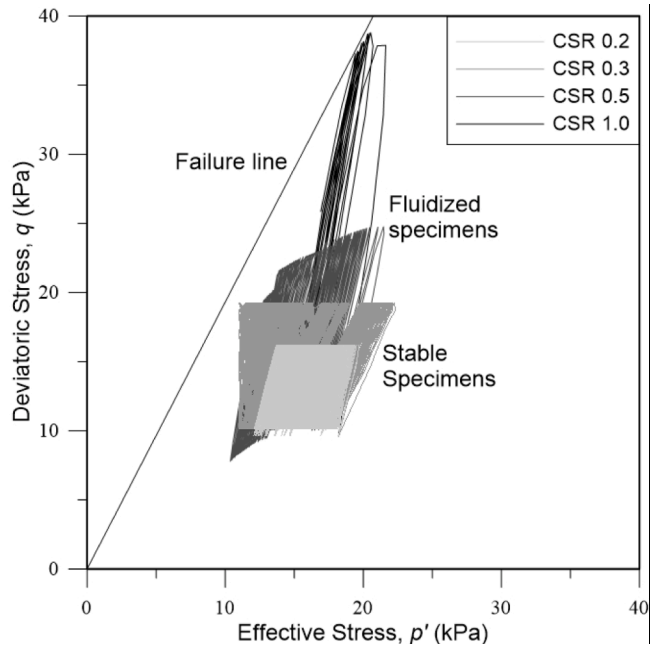

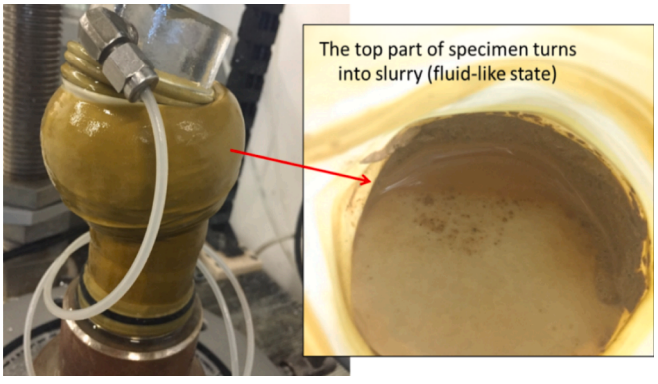

Fig. 5. Soil fluidisation under cyclic loading: a) stress paths (f = 1 Hz and ρ_d = 1790 kg/m^3); and b) observation of soil fluidisation, i.e., soil transformation into slurry (modified after [35]).

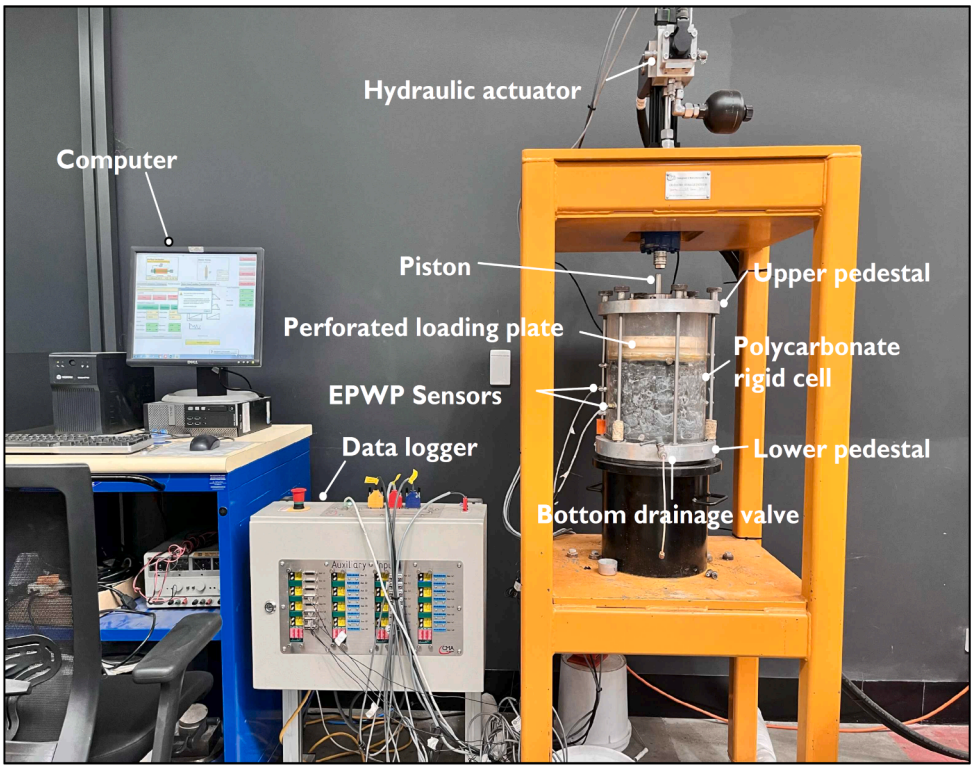

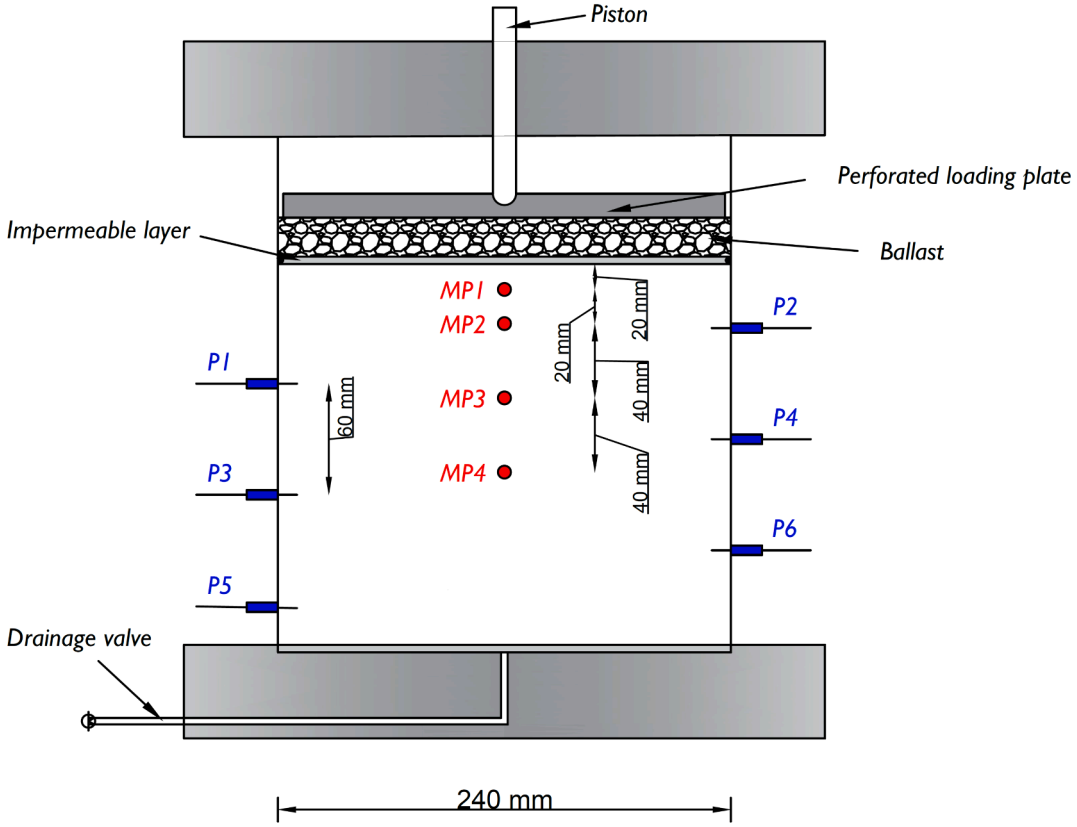

Fig. 6. Large-scale dynamic equipment to examine layered response of soil to cyclic loading (modified after [4;3]). Note: MP means miniature transducer for measuring pore water pressure.

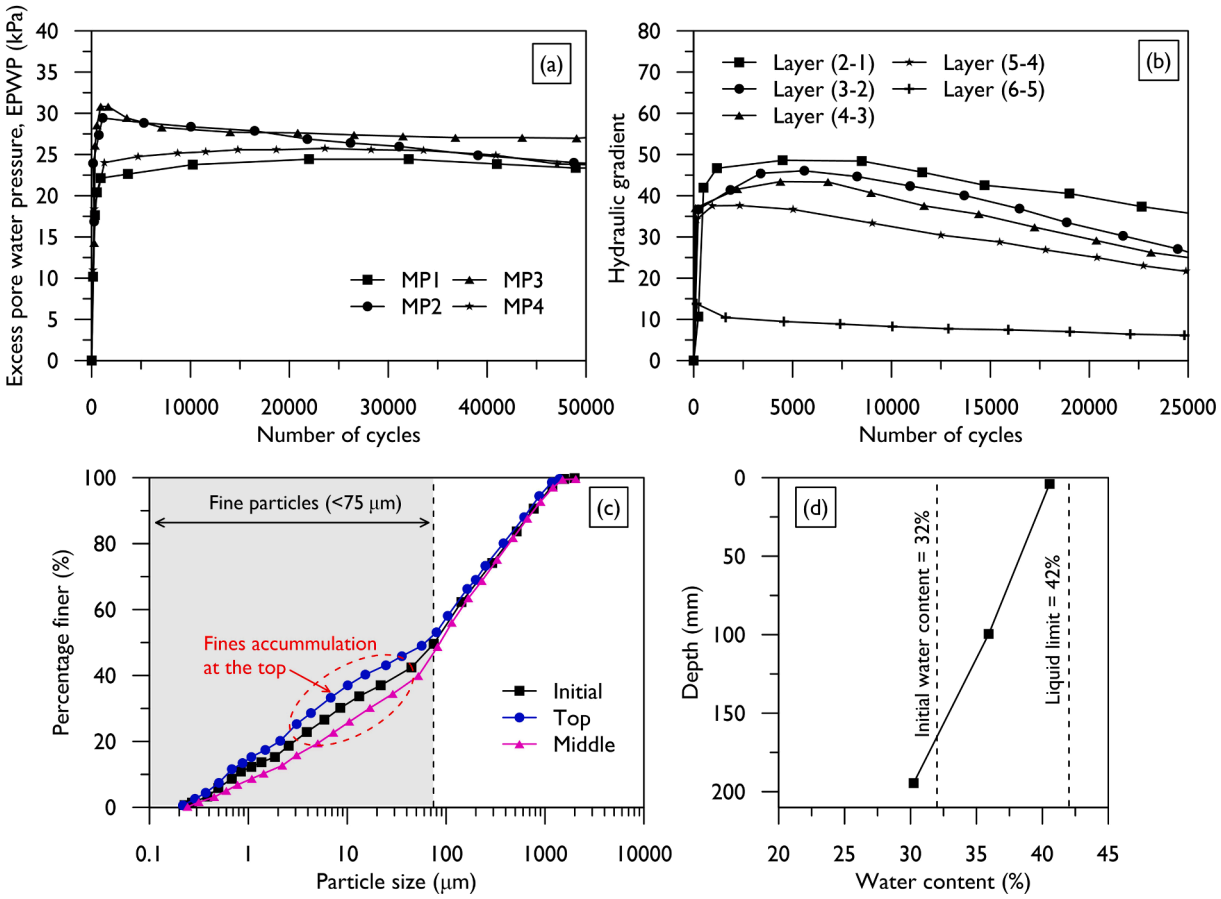

Fig. 7. Layered response of soil: a) Excess pore (water) pressure at different layers; and b) the corresponding interlayer pressure gradient; c) particle size distribution (PSD) and b) water content (modified after [4]).

compaction around 12 to 15 %, moist tamping was found to be the most convenient method for preparing the test specimens, and had the following advantages: (i) compaction could be applied in 10 different layers with a varying compaction energy intensity that enabled the desired initial density and uniform void ratio [38,35]; (ii) specimens were stable after tamping and less vulnerable to initial handling processes (e.g., unmoulded, transferring, membrane, positioning, etc) prior to loading. A recent study comparing consolidated and compacted specimens showed that moist tamping produced better-quality specimens [65].

The specimens were then placed onto the test frame and subjected to the following loading stages.

Stage 1 – Saturation and consolidation: The specimen was first flushed by de-aired water under an effective pressure of 5–10 kPa until no air bubbles can be seen from the drainage outlet. The cell and back pressures were increased simultaneously with a pressure difference of 10 kPa until the Skempton's B parameter exceeded 0.95. The soil specimen was then subjected to an anisotropic consolidation ratio of 0.6 (i.e., the effective horizontal stress divided by the effective vertical stress), representing a realistic in-situ stress state of subgrade soil. The initial mean effective stress was maintained at a relatively low level of 20 to 40 kPa.

Stage 2 – Cyclic loading: The loading frequency normally varied from 1 to 5 Hz to represent train speeds from 60-100 km/h. In triaxial contexts the cyclic stress ratio (CSR), which is the ratio between the applied deviator stress and twice the confining pressure, was considered to be the key parameter. Instead of the CSR, the vertical cyclic stress ratio (VCSR) and the torsional shear stress ratio (TSSR) were used to manipulate the stress state of soil in HC tests. A cyclic load was applied for 50,000 loading cycles or until failure. The definitions of VCSR and TSSR are given by:

$$VCSR = \Delta\sigma_z/(2 \times \sigma'_c) \quad (5)$$

$$\mathrm{TSSR} = \Delta\tau_{z\theta}/\sigma_z \quad (6)$$

where $\Delta\sigma_z$ and $\Delta\tau_{z\theta}$ are the applied vertical and torsional shear stresses; σ'_c is the effective confining pressure.

Key findings from laboratory testing

Instability of soil due to fluidisation under cyclic loading

A series of cyclic triaxial tests were carried out to examine the instability of soil induced by fluidisation [34,35,21]. The results showed that when soils were subjected to a certain combination of loading frequency (f) and cyclic stress ratio (CSR), an unstable state could be observed where the excess pore water pressure (EPWP) and axial strain increased rapidly. The key difference between this finding and past studies [62,45] is the internal migration of pore water along the soil specimen which caused the upper soil to fluidise (Fig. 5, this resulted in an increase in water content in the upper portion of soil as it approached the liquid limit (i.e., the liquidity index around unity). The specimens substantially deformed and were transformed into a slurry (fluid-like state); this was accompanied by a decrease in soil stiffness and a decrease in peak deviator stress (q). Fig. 5a shows that the maximum deviator stress can be sustained with almost constant or decreasing EPWP when the CSR is small (e.g., ≤ 0.5 for soil specimens with dry density $\rho_d = 1790$ kg/m^3). However, when the CSR exceeds a critical threshold (CSR_c), the soil faces early localised softening, especially at the top, and pushes pore water and fines to flow upward [52].

A large-scale test rig, namely the dynamic filtration apparatus [4],

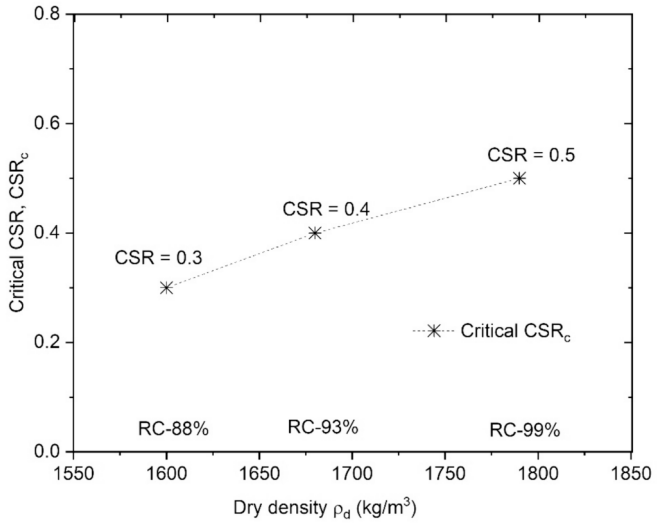

a)

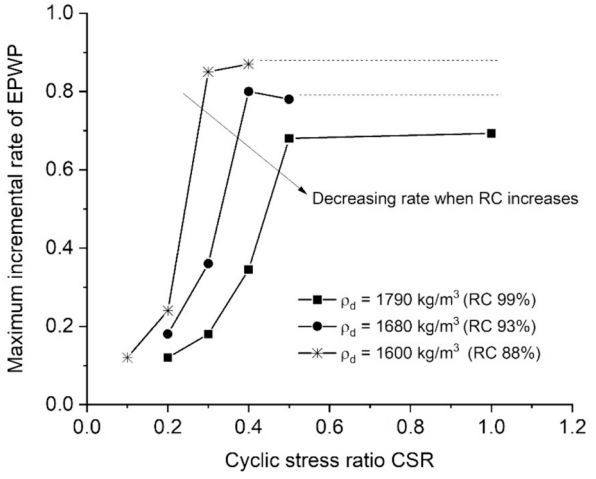

b)

Fig. 8. Influence of the degree of compaction on the instability of soil: a) change in critical CSR and number of cycles N_c with different RC values, b) incremental rate of EPWP with RC (modified after [35]).

was used to accommodate a larger soil sample (240 mm in diameter) so that localised measurements could be taken at different depths (Fig. 6). Four miniature transducers were installed vertically between 20 and 40 mm apart, together with six pore pressure sensors (P1 to P6) attached to the cell boundary. The cyclic load was applied using a hydraulic actuator acting through a piston and surface loading plate. The grain size distribution of tested soil had a clay percentage of 5 % (<5 μm), and a silt fraction of 45 % (5 < d < 74 μm). The liquid limit (LL) and plastic limit (PL) of the soil was 42 % and 26 %, respectively, thus the PI was 16. According to the Unified Soil Classification System (USCS), this soil could be classified as inorganic clay with medium plasticity. A vertical sinusoidal load with a minimum vertical stress of 30 kPa and a maximum vertical stress of 70 kPa was applied at a frequency of 5 Hz to represent the 25-ton axle loading of a heavy haul train travelling between 45–225 km/h [56,34]. Undrained subgrade conditions were replicated using an impermeable membrane at the subgrade-ballast interface.

As Fig. 7 shows, excess pore pressures rapidly develop during the first 500 cycles and remain above 22 kPa at the end of 50,000 cycles. The hydraulic gradients (the ratio between the pore pressure head difference and the distance between two locations) measured using body pressure transducers (P1-6) also show an increase in the gradient between the layers within the first 500 cycles, which then decreases with depth (Fig. 7b). For example, Layer (2–1) had a maximum gradient of 48 compared to only 15 in the bottom layer (Layer (6–5)). The larger hydraulic gradient implies that larger upward hydrodynamic forces act on the soil particles and induce fluidisation [49,52]. Furthermore, post-analysis of particle size distribution at three different locations, i.e., 0, 100, and 200 mm deep, were determined using the Malvern particle analyser (Fig. 7c). They show that fine particles (less than 75 μm) in the top part of the sample increased while the finer fraction decreases in the lower layers, implying an internal migration of fine particles. The water content measured at the top (near the ballast-subgrade interface) showed a considerable increase in water content from 32 % approaching the liquid limit (Fig. 7d), while that at the bottom layer remained closer to the initial value of 32 %.

Influence of compaction degree on cyclic response

The influence of compaction on the instability of soil under cyclic loading was carried out [35], where the soil specimens were prepared using the moist tamping method under three degrees of relative compaction (RC), i.e., 88 %, 93 % and 99 %. The optimum moisture content and maximum dry density were determined in accordance with ASTM standard [6]. These specimens were subjected to an identical cyclic load where the CSR was increased until soil failure occurred under an initial confining pressure of 15 kPa and a frequency of 1 Hz. The results showed that soil without sufficient compaction can be highly susceptible to fluidisation and instability. Fig. 8a shows how the critical value of CSR increases with larger degrees of RC. The CSR_c, which is the smallest value of CSR to trigger soil instability, increases from 0.3 to 0.5 when the RC increases from 88 % to 99 %. The results in Fig. 8b also show that the incremental rate of EPWP (i.e., the increment of EPWP per loading cycle) decreases by a factor of 2. For the same CSR, while the largest incremental rate of EPWP is 0.9 when RC = 88 %, it decreases to 0.65 when the RC increases to 99 %. This is because when soil is very dense, the dynamic EPWP developed inside porous space decreases significantly, while a larger load is shared by soil skeletons.

The role of soil plasticity in soil fluidisation

To increase the resistance to fluidisation, soil collected from a mud pumping site in NSW was mixed with 10 % and 30 % kaolin to change its plasticity [34]. Specifically, the collected soil was dried and broken into small particles before mixing with kaolin (dry powder) at the desired mass ratio (10 and 30 %). Distilled water was then sprayed to achieve a water content of 15 % during mixing. The mixture was sealed and stored in a humidity control room for 24 h to ensure uniform moisture distribution before making the test specimens. As a result, the PI increased from 11 % to 13 % and 15 % after mixing 10 % and 30 % kaolin by weight, respectively. Under the same initial dry density (1620 kg/m^3) and void ratio (0.64), cyclic triaxial tests with a confining pressure of 30 kPa (the anisotropic stress ratio $K = 0.6$) and loading frequency $f = 5$ Hz were applied to saturated undrained specimens. The results plotted in Fig. 9 show the original soil failed early at approximately 40 cycles, while the cyclic resistance increased to 135 cycles when 10 % kaolin was added. The measurement of water content along specimens showed that the difference in water content between the top and bottom of the specimens had decreased substantially due to the amount of kaolin and the high surface retention of clay particles which helped to mitigate soil fluidisation. However, when the amount of kaolin was too large, for example, 30 % in the current study, the soil could fail early due to shear failure.

Despite some previous studies examining the impact of clay content on the shear behaviour [54,66,48,19], the influence of mixing methods has not been adequately addressed. A recent study by Yin et al. [75]

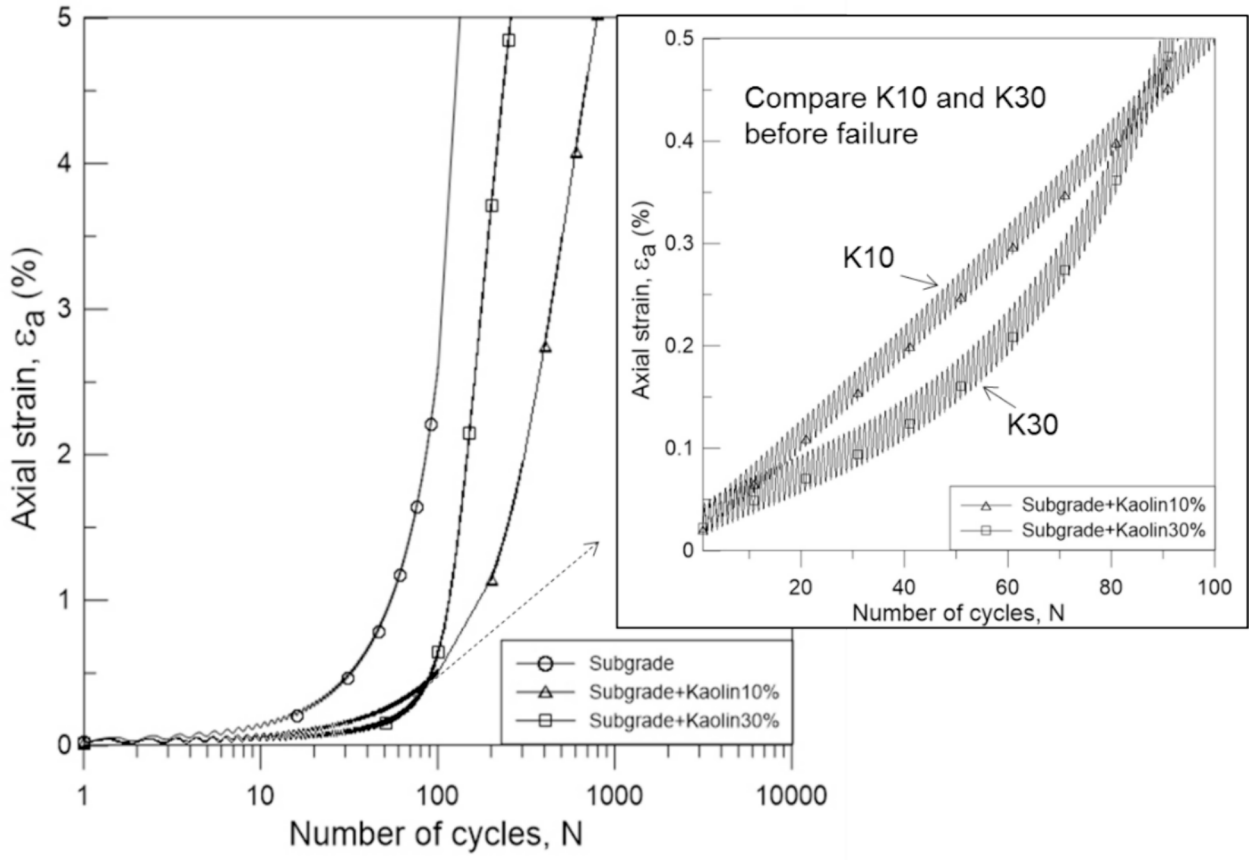

Fig. 9. Influence of the amount of kaolin on the cyclic response of soil (). reproduced from [35]

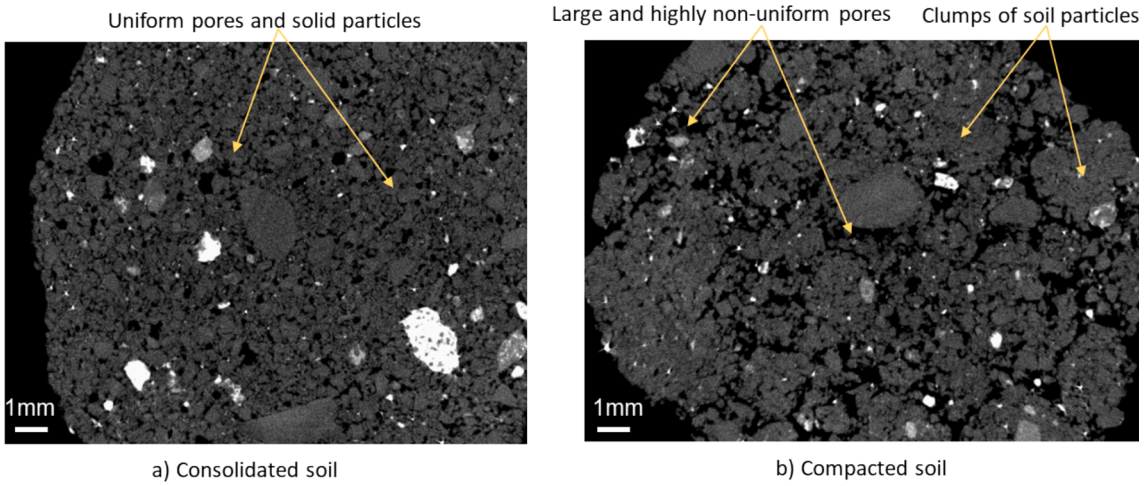

Fig. 10. Differences in soil fabric (arrangement of soil particles and pores) of specimens created by: a) consolidated and b) compacted methods under Micro-CT scanning.

examined three different mixing methods where the order of adding sand, clay and water was interchanged. Interestingly, these results showed that different mixing methods would affect the dispersion of clay particles within the soil matrix, thus altering its micro-pore characteristics. In the current study, the water was added after mixing the soil and kaolin powder to ensure consistency for all test specimens. Nevertheless, a comprehensive understanding of the influence of test specimen preparation methods on the shear behaviour needs further investigation.

Influence of soil fabric on cyclic response

The arrangement of soil particles and pores (soil fabric) can vary significantly in the field, depending on the stress state, formation history, and other factors. For example, subgrade layer under rail track can be formed by either compaction or the consolidation of natural soil. Silva et al. [65] studied how differences in soil fabric can affect the cyclic response of subgrade soil. Soil specimens were prepared by compaction and consolidation. Apart from the compaction method (moist tamping) described earlier, a 1D consolidation where slurry soil was consolidated

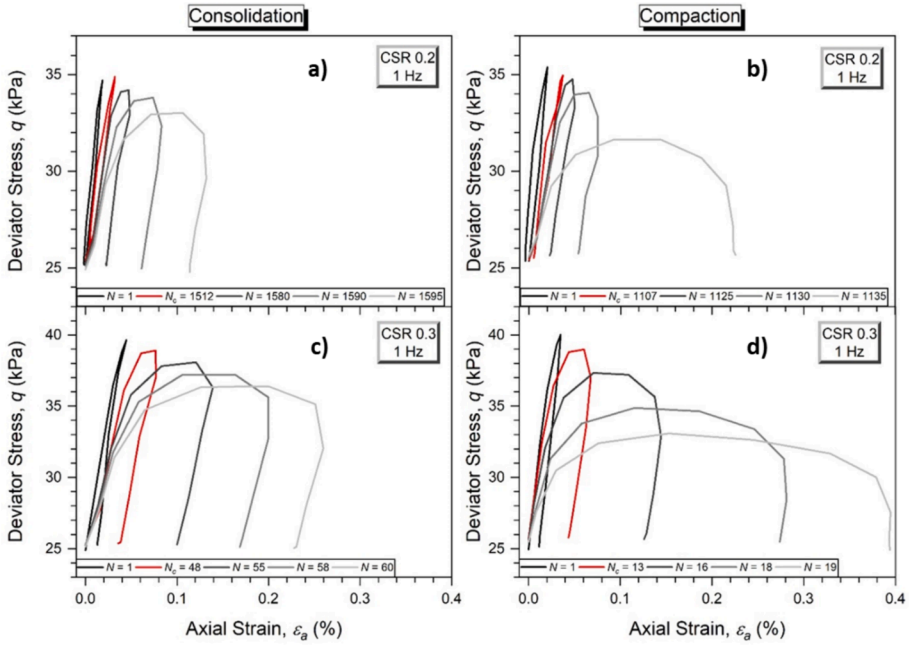

Fig. 11. Different responses of consolidated and compacted soils to 1 Hz cyclic loading: a & b) CSR = 0.2; c & d) CSR = 0.3;

under 50 kPa vertical stress was used. All the specimens had the same initial void ratio, i.e., approximately 0.66 (equivalent to a dry density of around 1700 kg/m^3). Based on the results of Micro-CT scanning, Fig. 10 shows very fine and uniform distributions of pores and soil particles for the consolidated specimen, whereas the compacted specimen had very large pores and clumps of soil. The 3D void structure shows that 60 % of the pores in consolidated soil were less than 67.4 μm in diameter, however, this d_{60} increased almost double to around 129 μm in the compacted soil.

Fig. 11 compares the cyclic responses of consolidated and compacted specimens under the same loading parameters (f = 1 Hz and CSR = 0.2 and 0.3). The results show that compacted soil tended to fail earlier than the consolidated soil. For example, for CSR = 0.2, the compacted soil experienced a very large increment of axial strain, i.e., 0.22 % at N = 1135 cycles, whereas the consolidated soil could still resist very well with less than 0.02 % at the same number of cyclic loadings. Furthermore, strain in the compacted specimen developed swiftly from approximately 0.05 % to 0.22 % within 5 cycles, i.e., from 1130 to 1135 cycles (Fig. 11b), but it happened more gently as the consolidated specimens failed. The consolidated soil only reached critical state (significant deformation) when N exceeded 1580 cycles. For the larger CSR (0.3), a similar trend was observed but at smaller thresholds of loading cycles.

Influence of stress rotation on cyclic instability of subgrade soil

Hollow cylinder (HC) tests were used to investigate how stress rotation can affect the response of soil to cyclic loading. A low plasticity soil (PI = 14) was compacted at a RC = 95 % to form test specimens. The HC test can control the principal stress angle and intermediate principal stress, thus enabling all the stress variables and states to be estimated. In addition to the vertical shear stress represented by the vertical cyclic stress ratio (VCSR) that is often considered in conventional triaxial tests, the torsional shear stress, including its magnitude TSSR and angle, could be manipulated depending on the intensity of stress rotation. Fig. 12 shows the correlation between the applied loading parameters and the stress components generated in the soil element. The cyclic vertical load and torque were controlled independently, while the external and internal confining pressures enabled the radial stresses to be established at an initial stage. This resulted in stress variations in vertical and circumferential directions of the soil element, as shown in Fig. 12; this changed the principal stresses which are functions of vertical, circumferential and shear stress variables. In the current study an effective confining pressure of 30 kPa and an initial deviator stress of 20 kPa (mean effective stress = 36.67 kPa) were established before cyclic loading. A loading frequency of 1 Hz was applied. The cyclic vertical shear stress was kept constant at 18 kPa (VCSR = 0.3), while the torsional shear stress was varied from 0 to 10.8 kPa (TSSR changed from 0 to 0.6 accordingly).

Fig. 13 shows the response of excess pore water pressure (EPWP) relative to the initial mean effective stress. Notably, TSSR = 0 represents no torsional shear stress, which is identical to the conventional triaxial tests. For the same VCSR = 0.3, EPWP only changes slightly when the TSSR varies from 0 to 0.4. In all cases the EPWP rises to a certain level and then stabilises. The largest EPWP ratio is around 0.2 when the TSSR is 0.4, but when the TSSR reaches 0.5 the EPWP develops substantially and accounts for more than 50 % of the initial mean effective stress (p') when N exceeds 10,000 cycles. The EPWP continues to increase until its ratio to p' reaches 0.55, which causes the specimen to fail (excessive deformation without the ability to resist loading). With a larger TSSR of 0.6, the EPWP rises abruptly during the first 50 cycles and then the specimen fails quickly at N = 150 cycles where the EPWP ratio = 0.55. These results indicate that the combined vertical and torsional shear stresses led to an earlier instability of soil compared to when only the vertical shear stress was considered. It is important to note that, findings from Gräbe and Clayton [22–23] shows that the effect of stress rotation lesser when the clay content of the material is higher.

Preventive measures for subgrade instability

Use of geocomposite to enhance drainage and filtration

The use of geosynthetics such as geotextiles and PVDs to enhance the drainage and filtration capacity of subgrade foundations has been reported as being an effective solution [1,13,3]. A proper geocomposite design can substantially alter the drainage of soil from undrained to partially or fully drained conditions. The buildup of EPWP can generate and dissipate, including slow to quick dissipations depending on the in-situ conditions, as well as the type and combination of geosynthetic

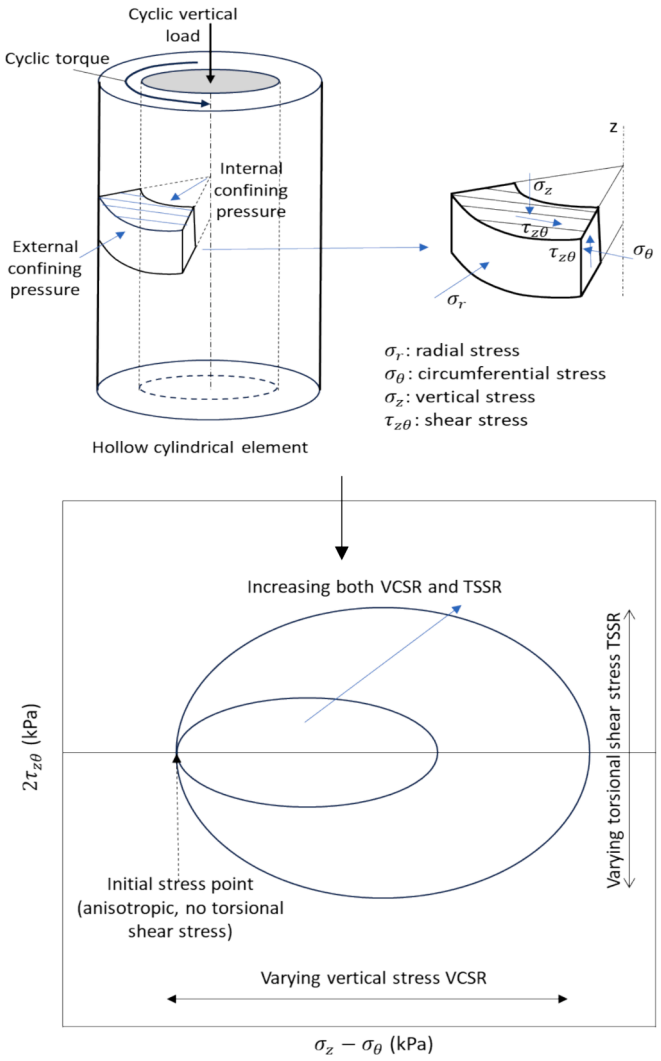

Fig. 12. Loading paths and corresponding stress components of hollow cylindrical soil specimen in vertical ($\sigma_z - \sigma_\theta$) and torsional $\tau_{z\theta}$ shear stress space.

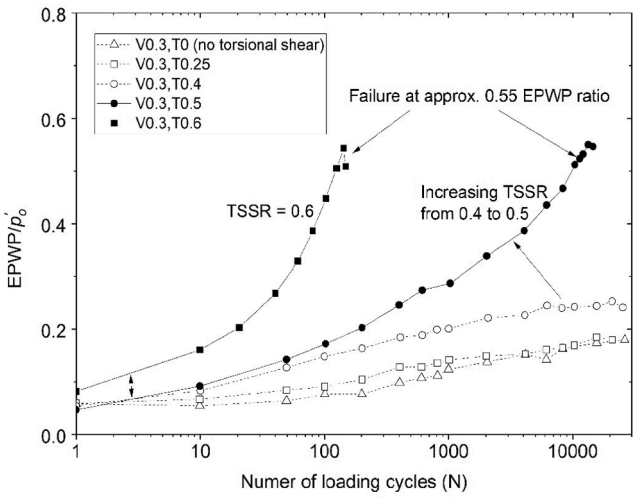

Fig. 13. Influence of combined vertical and torsional shear stresses on the accumulated excess pore water pressure (EPWP) and instability of subgrade soil. Note: EPWP is the excess pore water pressure; p_o' is the initial mean effective stress; V and T denote the vertical and torsional shear stress ratios VCSR and TSSR, respectively.

inclusions in the foundation [59,63,13]. Soil with low permeabilities, such as Australian soft estuarine clay which typically has a low permeability ($1.9x10^{-8}$ to $4.8x10^{-10}$ m/s) and a low coefficient of consolidation (typically around 2 m^2/year), usually experience a slow dissipation of excess pore pressure [53]. Geotextiles that are often applied onto the shallow layers have a limited effective depth of treatment, i.e., 1–2 m from the track surface. Moreover, past studies indicated potential clogging and a significant reduction in the permeability of surface geotextile due to ageing, resulting in the frequent occurrence of mud pumping in practice [8,63,10,51]. Past studies also showed that prefabricated vertical drains (PVDs) could be used to reduce the buildup of excess pore pressure in deeper subgrades [28,32]. For example, large-scale partially-drained triaxial tests by Indraratna et al. [29] with PVDs on kaolin samples showed a significant reduction in the buildup of excess pore pressure during cyclic loading, along with accelerated dissipation during rest periods. Furthermore, a field investigation [32] on the ability of PVDs to dissipate cyclic EPWP induced by train passage clearly proved they could stabilise subgrade soil under rail tracks.

A series of cyclic tests using dynamic filtration apparatus (shown earlier in Fig. 6) were conducted to facilitate the installation of geotextiles and PVDs in the same soil foundation. In these tests, four distinct cases were investigated:

(i) soil without geosynthetics (U);
(ii) soil with geotextiles (G),
(iii) soil with PVDs (P); and
(iv) soil with both geotextiles and PVD (i.e., geocomposite, P + G).

In the above, test (*i*) represents undrained conditions without any preventative measure that would serve as a reference to evaluate the efficiency of the other three solutions. Combinations of PVDs and geotextile can enhance cyclic resistance due to the presence of both drainage and filtration. The current study used a novel geotextile with pores in filter that were less than 1 μm. Notably, conventional geotextiles often have their apertures of around 50–100 μm which makes them vulnerable to clogging and a deteriorating performance.

The excess pore water pressure measured at 3 different depths in the specimens is shown in Fig. 14. The undrained test resulted in the highest EPWP of 30 kPa after 50,000 loading cycles with minimal dissipation. While the use of geosynthetics has shown reasonable dissipation of EPWP in overall, using geotextile (Test G) makes the EPWP rise to almost the same levels as in pure soil (Test U) due to the smaller discharge capacity induced by geotextiles compared to PVDs (i.e., longer drainage path). The EPWPs then dissipate and remain at approximately 15 kPa, i.e., 50 % from the initial peak at the end of test. The vertical drain reduces the accumulated EPWP by a substantial factor of 3, and when it is combined with a geotextile, this reduction factor rises to 6; for instance, the residual EPWP decreases from around 28 kPa (Test U) to about 5 kPa (Test P + G). Interestingly, the EPWP near the surface (MP1) for both Test P and Test G results in similar values at 50,000 cycles, but Test P results in a much lower peak excess pore pressure at the beginning. This indicates that for Test P, the rate of EPWP dissipation was higher during the initial stage of loading cycles than Test G, attesting to the outstanding performance of PVDs over geotextiles in enhancing the drainage capacity of soil foundation. On the other hand, the peak values of EPWP across different depths at 50,000 cycles in Test P + G were the lowest of the four tests. This proves that the combined PVD and geotextile (P + G) system is the best geosynthetics design for mitigating the potential for subgrade fluidisation during cyclic loading by effectively facilitating faster dissipation of EPWP.

Use of biopolymer to stabilising fluidised soil

Biopolymers such as Xanthan, Gellan, and Guar Gum are an emerging eco-friendly alternative to conventional cementation methods for stabilising soil such as lime and Portland cement. While most existing

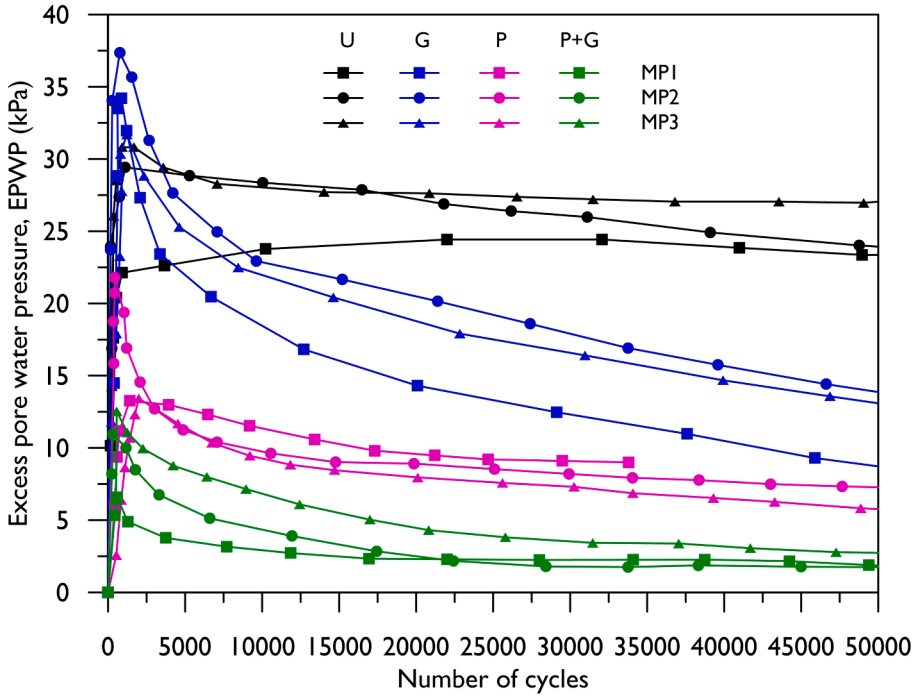

Fig. 14. Development of excess pore water pressure – Tests with Geocomposites (G), PVDs (P), PVD-Geocomposite system (P + G) and undrained (U) (modified after [3]).

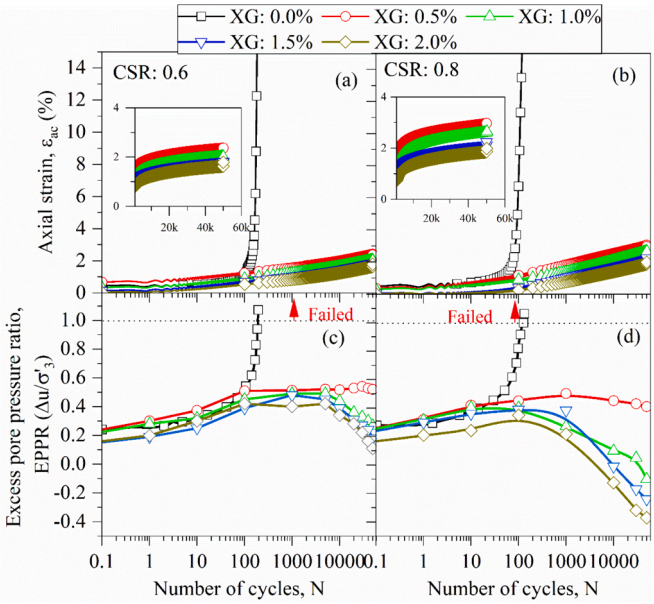

Fig. 15. Effects of biopolymer Xanthan Gum (XG) on the axial strain and excess pore water pressure of soil under CSR ().
reproduced from [21]

studies focus on soil behaviour under static loading conditions, our understanding of biopolymer-treated soil subjected to cyclic contexts is very limited [68,20]. A soil which was reported to be highly susceptible to mud pumping was used to examine the efficiency of using Xanthan Gum (XG) to enhance its resistance to fluidisation based on a cyclic triaxial test. Cyclic behaviour, including the localised distribution of internal moisture, was investigated for soil treated by the Xanthan Gum (XG) biopolymer. The amounts of XG varied from 0 to 2 % by mass, and the specimens of soil treated with biopolymer were cured in a conditional room at 25 °C for 28 days.

Fig. 15 shows the axial strain and corresponding EPWP behaviour (i.e., excess pore pressure ratio) of soil with and without XG treatment. Apparently, the specimens without XG fails at CSR = 0.6 and 0.8, and this is accompanied by a rapid increase in EWPW and excessive deformation. The specimens treated with XG could resist the cyclic loads very well because their EPWP ratios increases to around 0.4–0.5 and then decreases towards the end of the test. When subjected to a larger CSR, i.e., 0.8, the buildup of EPWP even become negative after 9000 cycles, indicating the appearance of dilatancy. With a small amount of XG, for example 0.5 %, the EPWP ratios rise to a peak of 0.5, but remain almost unchanged after 50,000 cycles. However, when the amount of XG > 0.5 %, the effect of biopolymer on the stabilisation of EPWP becomes even more pronounced. Corresponding to the stabilised EPWP, the axial strain of the specimens treated with XG develops rapidly but then slows down to an almost constant level at the end of the tests. The largest axial strain across all the treated specimens is at 3 % under CSR = 0.8; this showed excellent XG biopolymer performance in mitigating the settlement of soil under cyclic loading.

Fig. 16 shows the ability of biopolymer to mitigate the migration of internal pore water. When soil was not treated with a biopolymer, the pore water tended to migrate upward faster, making the water content in the upper part closer to the liquid limit (LL) and thus to experience soil fluidisation. By adding biopolymer, the water content at different positions within the specimen were almost identical (i.e., a liquidity index around 0.4–0.5). Visual observations confirmed that the soil specimens did not fluidise when treated with biopolymer; in fact, only 0.5 % XG could maintain a unform water content. Xanthan gum interacted with water (hydration) to form hydrogels that bonded the soil particles together and fill the porous space between them. This structural reinforcement not only enhanced the shear strength of soil it also prevented pore water from migrating upward under cyclic loading, thus mitigating soil fluidisation.

Conclusions

This paper has presented a selection of subgrade soil testing scenarios conducted recently by the UTS Transport Research Centre to provide an

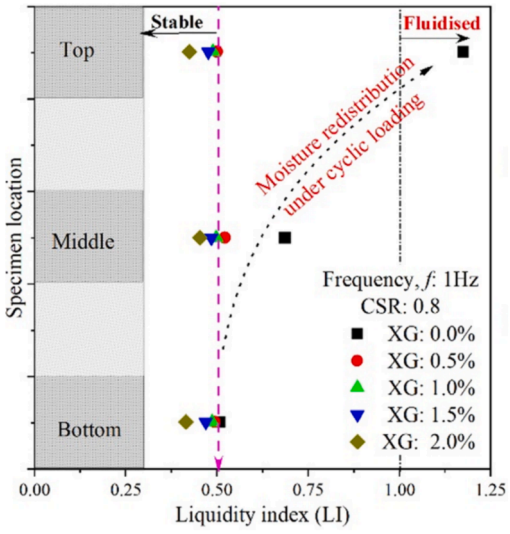

a)

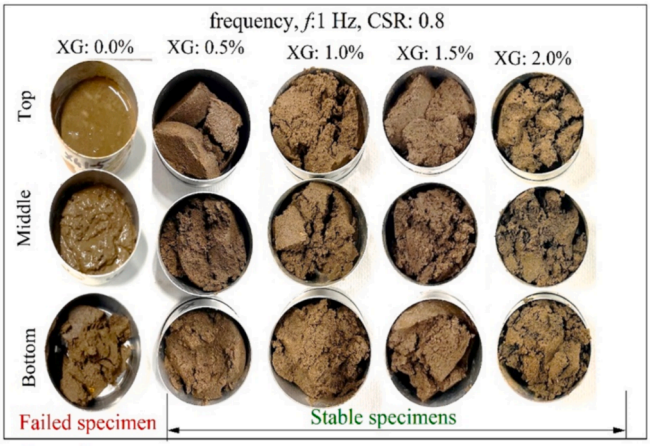

b)

Fig. 16. Examination of the water content along the specimens after cyclic tests: a) measured water content; and b) observation of soil specimens (). reproduced from [21]

insightful understanding of soft soil instability, with special reference to fluidisation (mud pumping). The salient findings reported in this paper and their implications lead to the following conclusions:

(i) Compared to the quasi-static response shown at relatively low speeds of less than 60 km/h, 3D FEM results indicated that the deviator stress in shallow subgrade layers could increase by factors of 1.2 and 2.0, when the train speed increased from 60 km/h to 120 and from 60 km/h to 240 km/h, respectively. These numerical findings further epitomised the importance of adopting appropriate ranges of stress magnitudes and frequencies in laboratory studies to simulate the actual field conditions.

(ii) Laboratory results pointed out the considerable internal migration of pore water in low to medium soil specimens under adverse cyclic loading, which caused a rapid increase in the water content and liquidity index (LI) within the upper soil region that triggered fluidisation. For instance, when a low plasticity soil (PI = 12–15) was compacted at 88 % of the maximum dry density, a cyclic loading with CSR = 0.3 and f = 1 Hz could cause hydraulic disequilibrium and stress localisation along specimen that resulted in upward migration of pore water and fine particles, thus resulting in structural or fabric degradation with the LI reaching unity at the top layer of the test specimen. Depending on the degree of compaction (e.g. RC = 93 %), a higher cyclic stress ratio (CSR > 0.4), can exacerbate localisation, leading to increased degradation of the soil fabric and the corresponding soil stiffness in the shallow subgrade layers. In a practical perspective, this leads to the conclusion that for a given axle load of train, the operating speeds must be controlled to prevent instability on tracks built over soft and saturated subgrade soils.

(iii) The cyclic instability of soil was governed by the degree of compaction, the clay content and plasticity index, as well as the soil fabric and loading characteristics. Soil with a relative compaction RC < 95 % can be vulnerable to instability, but increasing the clay content (e.g., 10 % kaolin content) can enhance its resistance to fluidisation. On the other hand, a much larger clay content in the proximity of 30 % could soften the subgrade soil considerably while sustaining higher excess pore water pressures, thus resulting in lower critical threshold of loading cycles that the soil can resist prior to plastic yielding.

(iv) The more uniform and integrated matrix that pores and soil particles could form, the larger the resistance to cyclic loading. For example, the consolidation process made the soil pores of the test specimen finer and better connected (d_{60} = 67.4 μm) than the test specimens subjected to compaction (d_{60} = 129 μm). This resulted in larger critical number of loading cycles (N_c = 1580 for consolidation compared to 1130 for compaction), given the same level of RC = 90 % for the same loading condition.

(v) Pronounced stress rotation caused by cyclic torsional shear (Hollow Cylinder Apparatus) can trigger soil instability at an earlier stage compared to the conventional cyclic triaxial testing where principal axes rotation is not possible. For instance, a soil compacted at RC = 95 % could effectively resist instability when only the vertical cyclic stress ratio VCSR = 0.3 was considered, but the same soil became unstable when subjected to a combined vertical (VCSR = 0.3) and torsional (TSSR ≥ 0.5) cyclic shear stress.

(vi) Prudent design using geocomposite can significantly enhance the performance of soft subgrade under cyclic loading. Micropore-geotextiles was found to be highly resilient to clogging induced by migrating fines, while the combination of PVD and geotextiles further improved the internal soil stability by reducing the rate of EPWP increase during cyclic loading.

(vii) The research outcomes also attested to the promising potential of using eco-friendly biopolymer to improve the cyclic resistance of soft subgrade soil, especially in relation to mitigating fluidisation. Only a very small quantity (0.5 %) of Xanthan Gum was required to substantially reduce the internal migration of pore water under cyclic loading, thus providing a more stable soil matrix resisting fluidisation.

CRediT authorship contribution statement

Buddhima Indraratna: Writing – review & editing, Supervision, Resources, Project administration, Methodology, Investigation, Funding acquisition, Conceptualization. **Thanh T. Nguyen:** Writing – original draft, Investigation, Formal analysis. **Shashika Atapattu:** Writing – original draft, Methodology, Investigation, Formal analysis. **Trung Ngo:** Writing – original draft, Validation, Methodology, Formal analysis. **Cholachat Rujikiatkamjorn:** Writing – review & editing, Methodology.

Declaration of competing interest

The authors declare the following financial interests/personal relationships which may be considered as potential competing interests: This research was funded by Transport Research Centre (TRC), UTS and

Australian Research Council (ARC, LP160101254 and DE230101127).

Data availability

Data will be made available on request.

Acknowledgements

The extensive research reported in this paper could not be implemented without robust support from various industry partners such as Sydney Trains, ACRI, SMEC, Coffey, ARTC (Australian Rail Track Corporation), among others. The financial support from Australian Research Council (LP160101254 and DE230101127) and Transport Research Centre (TRC, UTS) are grateful. Contributions from various past and current PhD students such as Dr Ameyu Tucho, Dr Ramesh Gedela, Dr Joseph Arivalagan, Dr Warrantorn Korkitsuntornsan, Dr Mandeep Singh, Dr Aruni Abeywickrama, Ms Isabella Novais Silva and Ms Lakshmi Nair through their theses at UOW and UTS are much appreciated.

References

[1] Alobaidi I, Hoare DJ. Qualitative criteria for anti-pumping geocomposites. Geotext Geomembr 1998;16(4):221–45.
[2] Ansal A, Erken A. Undrained behavior of clay under cyclic shear stresses. J Geotech Eng 1989;115(7):968–83.
[3] Arivalagan J, Indraratna B, Rujikiatkamjorn C, Warwick A. Effectiveness of a Geocomposite-PVD system in preventing subgrade instability and fluidisation under cyclic loading. Geotext Geomembr 2022;50(4):607–17.
[4] Arivalagan J, Rujikiatkamjorn C, Indraratna B, Warwick A. The role of geosynthetics in reducing the fluidisation potential of soft subgrade under cyclic loading. Geotext Geomembr 2021;49(5):1324–38.
[5] Arulrajah, A., Abdullah, A., Bo, M.W. & Bouazza, A. 2009, 'Ground improvement techniques for railway embankments', *Proceedings of the Institution of Civil Engineers - Ground Improvement*, vol. 162, no. 1, pp. 3–14, viewed 27 January 2023, <https://www.icevirtuallibrary.com/doi/10.1680/grim.2009.162.1.3>.
[6] Astm. D698. Standard Test Methods for Laboratory Compaction Characteristics of Soil Using Standard Effort. West Conshohocken, PA: ASTM International; 2007.
[7] Atapattu, S., Indraratna, B. & Rujikiatkamjorn, C. 2023, 'Influence of periodic cyclic loading and rest period on soft clay consolidation', *Proceedings of the Institution of Civil Engineers: Ground Improvement*, vol. 177, no. 1, pp. 30–43.
[8] Aw, E.S. 2007, *Low Cost Monitoring System to Diagnose Problematic Rail Bed: Case Study at a Mud Pumping Site*, no. 2001, p. 203.
[9] Bian X, Jiang H, Cheng C, Chen Y, Chen R, Jiang J. Full-scale model testing on a ballastless high-speed railway under simulated train moving loads. Soil Dyn Earthq Eng 2014;66:368–84.
[10] Bruzek, R., Stark, T.D., Wilk, S.T., Thompson, H.B. & Sussmann Jr, T.R. 2016, 'Fouled ballast definitions and parameters', *ASME/IEEE Joint Rail Conference*, vol. 49675, American Society of Mechanical Engineers, p. V001T01A007.
[11] Cai Y, Chen Y, Cao Z, Ren C. A combined method to predict the long-term settlements of roads on soft soil under cyclic traffic loadings. Acta Geotech 2018;13(5):1215–26.
[12] Chai J-C, Miura N. Traffic-Load-Induced Permanent Deformation of Road on Soft Subsoil. J Geotech Geoenviron Eng 2002;128(11):907–16.
[13] Chawla S, Shahu JT. Reinforcement and mud-pumping benefits of geosynthetics in railway tracks: Model tests. Geotext Geomembr 2016;44(3):366–80.
[14] Connolly D, Giannopoulos A, Forde MC. Numerical modelling of ground borne vibrations from high speed rail lines on embankments. Soil Dyn Earthq Eng 2013;46:13–9.
[15] Correia AG, Cunha J. Analysis of nonlinear soil modelling in the subgrade and rail track responses under HST. Transp Geotech 2014;1(4):147–56.
[16] Ding Y, Jia Y, Zong Z, Wang X, Zhang J, Chen X. Study on characteristics and mechanism of subgrade mud pumping under heavy-haul train loads. Bull Eng Geol Environ 2024;83(2):1–17.
[17] Duong TV, Cui Y-J, Tang AM, Dupla J-C, Canou J, Calon N, et al. Investigating the mud pumping and interlayer creation phenomena in railway sub-structure. Eng Geol 2014;171:45–58.
[18] Esveld C. Modern railway track, vol. 385. MRT-productions Zaltbommel; 2015.
[19] Fedakar HI, Cetin B, Rutherford CJ. Deformation characteristics of medium-dense sand-clay mixtures under a principal stress rotation. Transp Geotech 2021;vol. 30, no. July:100616.
[20] Gedela R, Indraratna B, Medawela S, Nguyen TT. Effects of fines content on the strength and stiffness of biopolymer treated low-plasticity soils. Aust Geomech J 2023.
[21] Gedela R, Indraratna B, Nguyen TT, Medawela S. The effect of biopolymer treatment on the potential instability of a soft soil under cyclic loading. Transp Geotech 2023;42:101102.
[22] Gräbe PJ, Clayton CR. Effects of Principal Stress Rotation on Permanent Deformation in Rail Track Foundations. J Geotech Geoenviron Eng 2009;135(4):555–65.
[23] Gräbe PJ, Clayton CRI. Effects of Principal Stress Rotation on Resilient Behavior in Rail Track Foundations. J Geotech Geoenviron Eng 2014;140(2):555–65.
[24] Guo L, Cai Y, Jardine RJ, Yang Z, Wang J. Undrained behaviour of intact soft clay under cyclic paths that match vehicle loading conditions. Can Geotech J 2018;55(1):90–106.
[25] Hall L. Simulations and analyses of train-induced ground vibrations in finite element models. Soil Dyn Earthq Eng 2003;23(5):403–13.
[26] Huang J, Su Q, Liu T, Wang W. Behavior and control of the ballastless track-subgrade vibration induced by high-speed trains moving on the subgrade bed with mud pumping. Shock Vib 2019;2019.
[27] Huang J, Wang J, Lv Y, Cai X, Chen J, Fu X, et al. Influences of Cyclic Confining Pressure on Deformation Behaviors of Soft Clay under Intermittent Cyclic Loading. Int J Geomech 2024;24(4):1–11.
[28] Indraratna B, Attya A, Rujikiatkamjorn C. Experimental Investigation on Effectiveness of a Vertical Drain under Cyclic Loads. J Geotech Geoenviron Eng 2009;135(6):835–9.
[29] Indraratna B, Korkitsuntornsan W, Nguyen TT. 2020a, 'Influence of Kaolin content on the cyclic loading response of railway subgrade'. Transp Geotech 2019;22(August):100319.
[30] Indraratna B, Ngo T, Ferreira FB, Rujikiatkamjorn C, Tucho A. Large-scale testing facility for heavy haul track. Transp Geotech 2021;vol. 28, no. January:100517.
[31] Indraratna B, Nimbalkar S, Christie D, Rujikiatkamjorn C, Vinod J. Field Assessment of the Performance of a Ballasted Rail Track with and without Geosynthetics. J Geotech Geoenviron Eng 2010;136(7):907–17.
[32] Indraratna B, Rujikiatkamjorn C, Ewers B, Adams M. Class A Prediction of the Behavior of Soft Estuarine Soil Foundation Stabilized by Short Vertical Drains beneath a Rail Track. J Geotech Geoenviron Eng 2010;136(5):686–96.
[33] Indraratna B, Salim W, Rujikiatkamjorn C. Advanced rail geotechnology - Ballasted track. Advanced Rail Geotechnology - Ballasted Track 2011.
[34] Indraratna B, Singh M, Nguyen TT. The mechanism and effects of subgrade fluidisation under ballasted railway tracks. Railway Engineering Science 2020;28(2):113–28.
[35] Indraratna B, Singh M, Nguyen TT, Leroueil S, Abeywickrama A, Kelly R, et al. Laboratory study on subgrade fluidization under undrained cyclic triaxial loading. Can Geotech J 2020;57(11):1767–79.
[36] El Kacimi A, Woodward PK, Laghrouche O, Medero G. Time domain 3D finite element modelling of train-induced vibration at high speed. Comput Struct 2013;118:66–73.
[37] Kouroussis G, Van Parys L, Conti C, Verlinden O. Using three-dimensional finite element analysis in time domain to model railway-induced ground vibrations. Adv Eng Softw 2014;70:63–76.
[38] Ladd RS. Specimen preparation and liquefaction of sands. J Geotech Eng Div 1974;100(10):1180–4.
[39] Lei H, Liu M, Feng S, Liu J, Jiang M. Cyclic Behavior of Tianjin Soft Clay under Intermittent Combined-Frequency Cyclic Loading. Int J Geomech 2020;20(10):1–10.
[40] Leng W, Xiao Y, Nie R, Zhou W, Liu W. Investigating Strength and Deformation Characteristics of Heavy-Haul Railway Embankment Materials Using Large-Scale Undrained Cyclic Triaxial Tests. Int J Geomech 2017;17(9):1–13.
[41] Li D, Selig ET. Evaluation of railway subgrade problems. Transp Res Rec 1995;1489:17–25.
[42] Li D, Selig ET. Cumulative Plastic Deformation for Fine-Grained Subgrade Soils. J Geotech Eng 1996;122(12):1006–13.
[43] Li D, Selig ET. Method for Railroad Track Foundation Design. I: Development. J Geotech Geoenviron Eng 1998;124(4):316–22.
[44] Li Y, Nie R, Guo Y, Wang C, Wang Q, Yue Z. 2023, 'Resilient deformation characteristics of subgrade silty filler under intermittent train loading'. Transp Geotech 2023;40(November):100952.
[45] Liu J, Xiao J. Experimental Study on the Stability of Railroad Silt Subgrade with Increasing Train Speed. J Geotech Geoenviron Eng 2010;136(6):833–41.
[46] Lu X, Kim C-W, Chang K-C. Finite element analysis framework for dynamic vehicle-bridge interaction system based on ABAQUS. Int J Struct Stab Dyn 2020;20(03):2050034.
[47] Mamou A, Powrie W, Priest JA, Clayton C. The effects of drainage on the behaviour of railway track foundation materials during cyclic loading. Geotechnique 2017;67(10):845–54.
[48] Mamou A, Priest JA, Clayton CRI, Powrie W. Behaviour of saturated railway track foundation materials during undrained cyclic loading. Can Geotech J 2018;55(5):689–97.
[49] Nguyen TT, Indraratna B. Fluidization of soil under increasing seepage flow: an energy perspective through CFD-DEM coupling. Granul Matter 2022;24(3):80.
[50] Nguyen TT, Indraratna B. Rail track degradation under mud pumping evaluated through site and laboratory investigations. International Journal of Rail Transportation 2022;10(1):44–71.
[51] Nguyen TT, Indraratna B, Kelly R, Phan NM, Haryono F. Mud pumping under railtracks: Mechanisms, assessments and solutions. Aust Geomech J 2019;54(4):59–80.
[52] Nguyen TT, Indraratna B, Leroueil S. Localized behaviour of fluidized subgrade soil subjected to cyclic loading. Can Geotech J 2022;59(10):1844–9.
[53] Pineda, J.A., Liu, X.F. & Sloan, S.W. 2016, 'Effects of tube sampling in soft clay: A microstructural insight', *Geotechnique*, vol. 66, no. 12, pp. 969–83, viewed 10 October 2022, <https://doi.org/10.1680/jgeot.15.P.217]>.

[54] Polito CP, Martin JR. Effects of Nonplastic Fines on the Liquefaction Resistance of Sands. J Geotech Geoenviron Eng 2001;127(5):408–15.
[55] Powrie W, Le Pen L, Milne D, Thompson D. Train loading effects in railway geotechnical engineering: Ground response, analysis, measurement and interpretation. Transp Geotech 2019;vol. 21, no. July:100261.
[56] Powrie W, Yang LA, Clayton CRI. Stress changes in the ground below ballasted railway track during train passage. Proceedings of the Institution of Mechanical Engineers, Part F: Journal of Rail and Rapid Transit 2007;221(2):247–61.
[57] Priest JA, Powrie W, Yang L, Grabe PJ, Clayton CRI. Measurements of transient ground movements below a ballasted railway line. Geotechnique 2010;60(9):667–77.
[58] Raymond GP. Geotextile application for a branch line upgrading. Geotext Geomembr 1986;3(2–3):91–104.
[59] Sakai A, Samang L, Miura N. Partially-drained cyclic behavior and its application to the settlement of a low embankment road on silty-clay. Soils Found 2003;43(1):33–46.
[60] Saleeb AF, Kumar A. Automated finite element analysis of complex dynamics of primary system traversed by oscillatory subsystem. Int J Comput Methods Eng Sci Mech 2011;12(4):184–202.
[61] Sayeed MA, Shahin MA. Three-dimensional numerical modelling of ballasted railway track foundations for high-speed trains with special reference to critical speed. Transp Geotech 2016;6:55–65.
[62] Selig, E.T. & Waters, J.M. 1994, *Track geotechnology and substructure management*, Thomas Telford.
[63] Sharpe P, Roskams T, Valero SN. The development of a geocomposite to prevent mud pumping. In: Proceedings of the 2014 Conference on Railway Excellence: Rail Transport for Vital Economy. Railway Technical Society of Australasia (RTSA); 2014. p. 346–53.
[64] Shih J-Y, Thompson DJ, Zervos A. The effect of boundary conditions, model size and damping models in the finite element modelling of a moving load on a track/ground system. Soil Dyn Earthq Eng 2016;89:12–27.
[65] Silva IN, Indraratna B, Nguyen TT, Rujikiatkamjorn C. The influence of soil fabric on the monotonic and cyclic shear behaviour of consolidated and compacted specimens. Can Geotech J 2023:1–44.
[66] Simpson DC, Evans TM. Behavioral Thresholds in Mixtures of Sand and Kaolinite Clay. J Geotech Geoenviron Eng 2016;142(2):1–10.
[67] Singh M, Indraratna B, Nguyen TT. Experimental insights into the stiffness degradation of subgrade soils prone to mud pumping. Transp Geotech 2021;27:100490.
[68] Soldo A, Miletić M, Auad ML. Biopolymers as a sustainable solution for the enhancement of soil mechanical properties. Sci Rep 2020;10(1):267.
[69] Sun QD, Indraratna B, Nimbalkar S. Deformation and degradation mechanisms of railway ballast under high frequency cyclic loading. J Geotech Geoenviron Eng 2016;142(1):4015056.
[70] Tong J, Wu T, Guo L, Yuan Z, Jin H. Long-term cyclic behavior of soft clay under different variable confining pressures and partially drained conditions. Transp Geotech 2022;33:100723.
[71] Truong MH, Indraratna B, Nguyen TT, Carter J, Rujikiatkamjorn C. 2021, 'Analysis of undrained cyclic response of saturated soils'. Comput Geotech 2021;134(July):104095.
[72] Tucho A, Indraratna B, Ngo T. Stress-deformation analysis of rail substructure under moving wheel load. Transp Geotech 2022;36:100805.
[73] Wang K, Zhuang Y. Characterizing the permanent deformation Response-Behavior of subgrade material under cyclic loading based on the shakedown theory. Constr Build Mater 2021;311(2):125325.
[74] Xiao J, Juang CH, Wei K, Xu S. Effects of Principal Stress Rotation on the Cumulative Deformation of Normally Consolidated Soft Clay under Subway Traffic Loading. J Geotech Geoenviron Eng 2014;140(4):1–9.
[75] Yin, K., Fauchille, A.-L., Di Filippo, E., Othmani, K., Branchu, S., Sciarra, G. & Kotronis, P. 2021, 'The Influence of Mixing Orders on the Microstructure of Artificially Prepared Sand-Clay Mixtures', Y. Jia (ed.), Adv Mater Sci Eng, vol. 2021, pp. 1–15.